Experiment on a Double-Foot Stepping Piezoelectric Linear Motor

Sun Mengxin[1], *Huang Weiqing*[1,2*], *Wang Yin*[3], *Lu Qian*[1]

1. State Key Laboratory of Mechanics and Control of Mechanical Structures, College of Aerospace Engineering, Nanjing University of Aeronautics and Astronautics, Nanjing 210016, P. R. China
2. School of Mechanical and Electric Engineering, Guangzhou University, Guangzhou 510006, P. R. China
3. Center for Precision Measurement Technologies and Instruments, Huaqiao University, Xiamen 361021, P. R. China

(Received 18 October 2016; revised 12 January 2017, accepted 19 January 2017)

Abstract: A novel double-foot piezoelectric linear motor is proposed. The kinematic model of the motor under stepping motion is presented. The motor mainly consists of a stator with four piezoelectric stacks, a mover, a holding mechanism, and a preloading mechanism to achieve large stroke with high resolution. Finite element simulations are carried out to analyze the motion characteristics of the motor. A prototype is fabricated and a serial experiments are conducted to validate the feasibility of the motor principle. Experimental results indicate that the motor can move at a speed of 670.22 μm/s with a driving frequency of 120 Hz and a voltage of 120 V. The resolution of the proposed motor is 3.6 μm while the resolution of the single-step motion is 0.1 μm.

Key words: piezoelectric linear motor; piezoelectric stack; performance test

CLC number: O241.6 **Document code**: A **Article ID**: 1005-1120(2018)03-0423-09

0 Introduction

Taking advantages of simple structure, high precision, quick response as well as low power consumption, piezoelectric linear motors have shown wide application prospect[1-4]. These motors can be classified into resonant and non-resonant types by vibration mode. Resonant piezoelectric motor is a conventional type with the advantages of flexible design, high load capacity and small size[5, 6]. The main disadvantages of this type is that motion of the motor would be unstable as the system must work under resonance state which is used to amplify the displacement of driving element and it will be easily affected by the environment. When the working frequency of the system has small difference with the resonant frequency, it may cause obvious fluctuation in the performance of motor[7]. Non-resonant piezoelectric motors utilize the piezoelectric stack as the core driving element. Since the piezoelectric motor can output a large displacement with small driving voltage, the motor will work stably without resonant state.

Various kinds of piezoelectric actuators with piezoelectric stack have been developed by previous researchers. The inchworm motor[8, 9] and inertial motor[10-12] are two important categories among them. The inchworm motor is a kind of bionic motor with the advantages of strong loading capacity and high precision accuracy. The device usually has the drawback of complex structure and assembling. Another type of motor based on inertial driving principle often has a high holding and a high pushing force. However, it puts forward high demands on driving signal and control system.

According to the different ways of producing linear motion, the work modes of non-resonant piezoelectric motors can be classified into three

* Corresponding author, E-mail address: mehwq@nuaa.edu.cn.

How to cite this article: Sun Mengxin, Huang Weiqing, Wang Yin, et al. Experiment on a double-foot stepping piezoelectric linear motor[J]. Trans. Nanjing Univ. Aero. Astro., 2018,35(3):423-431.
http://dx.doi.org/10.16356/j.1005-1120.2018.03.423

categories, i. e., straight moving mode, step actuation mode, and continuous actuation mode. In straight moving mode, a movement is generated by pushing the mover with force of piezoelectric stack itself. The motor with this mode has the drawback of limited stroke. The motor with step actuation mode usually achieves large stroke and operates in a quasi-static mode. However, these motors always have complex mechanism and high demands on fabrication. When a driving signal with high frequency is applied to the motor, the motor will work in a continuous actuation mode. The high frequency drive power supply for this mode is a technical bottleneck as piezoelectric stack has high capacitance. On the basis of existing research on non-resonant piezoelectric motor[13-16], a step actuation mode linear motor is designed and it is aimed to achieve large stroke and high resolution on one motor to meet the increasing industrial demand of precision linear feed system.

1 Design and Analysis

1.1 Motor structure

The model of non-resonant piezoelectric linear motor driving by double-foot is shown in Fig. 1. It consists of a stator, a mover, a holding mechanism, and a preloading mechanism. In this motor, the stator encompasses four piezoelectric stacks which are divided into two groups setting in two layer structures of the stator. The mover is the output element of the motor. The holding device is fixed at one side of the stator which has played an important role in positioning, and the preloading device is set at the other side of the stator to provide enough preload force to guarantee the stable contact between the stator and the mover.

The guide mechanism and preload structure matching the above stator are designed as shown in Fig. 2.

The holding device consists of a stator box, a guide mechanism (three adjusting blocks, two connecting pieces and one preset beam) and a

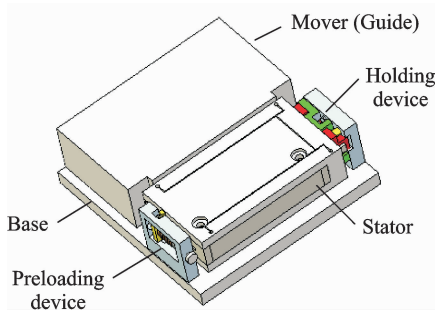

Fig. 1 Structure model of motor

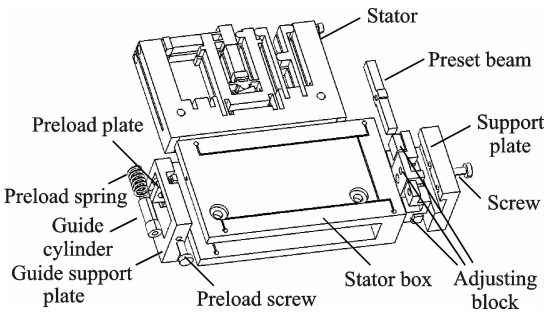

Fig. 2 Explode diagram of motor structure

support plate. The stator box is used to limit the movement of the stator in horizontal and out of plane directions and keep the degree of freedom of the stator in longitudinal direction. Adjust the guide mechanism to make sure the surface of stator top contact the mover completely when assembling. The preload structure consists of a guide cylinder, a preload screw, a preload plate, a spring and a guide support plate. Using the preload screw to make the guide cylinder and the spring compress the support plate. Thus the preload force between the stator and the mover is provided by this way.

1.2 Mechanism analysis

As the stator is the input element and core component of the motor, it has a vital influence on performance of the motor, the design of the stator is particularly important. The stator consists of two-layer structures. One-layer structure of the stator is shown in Fig. 3.

Kinematics model of the layer structure is set up as shown in Fig. 4, where m_1 is the mass of the top of driving foot, m_{21} and m_{22} are the mass of upper part of the flexure hinge and the piezoe-

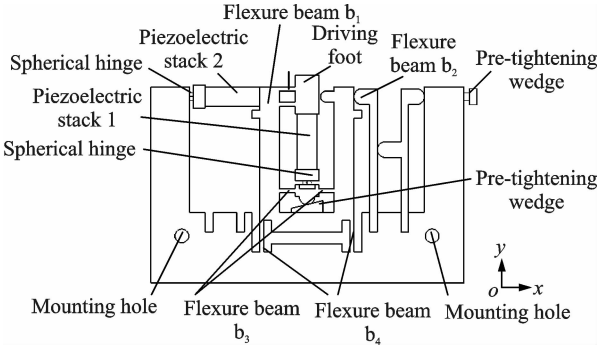

Fig. 3 Layer structure of stator

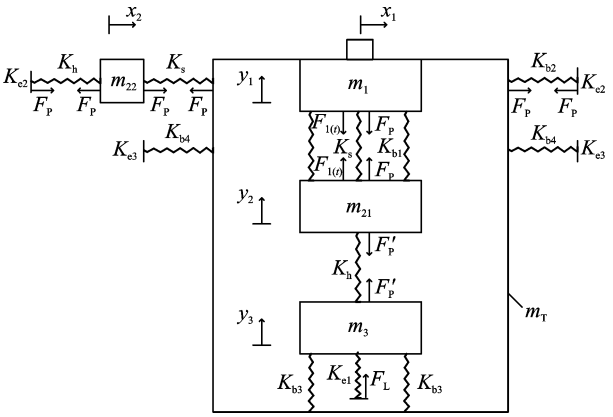

Fig. 4 Kinematics model of stator

lectric stacks 1 and 2, m_3 is the mass of lower part of the flexure hinge and the elastic beam, K_s is the stiffness of stack, K_h is the stiffness of flexure hinge, K_{b1}, K_{b2}, K_{b3}, K_{b4} are the equivalent stiffnesses of the elastic beams 1, 2, 3, 4, and K_{e1}, K_{e2}, K_{e3} are the equivalent stiffnesses of the external structure. F_h is the initial force of the hinge, F_h the preload force applied on stack, $F_1(t)$, $F_2(t)$ the output forces of stack, and F_2

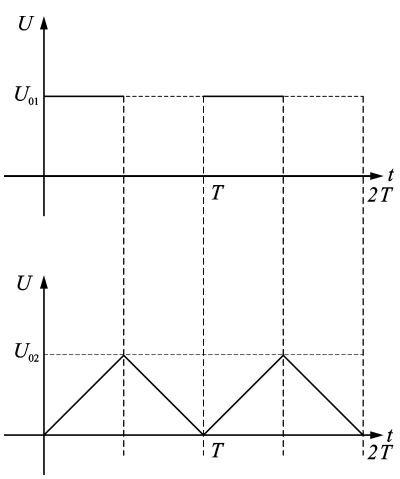

Fig. 5 Input signal applied on stack of y and x directions

the force of screw. The voltage signal in Fig. 5 is applied on the stacks of y and x directions. This signal can be derived as

y direction

$$U_1(t)=\begin{cases}U_{01} & 0\leqslant (t \bmod T)\leqslant \dfrac{T}{2}\\ 0 & \dfrac{T}{2}<(t \bmod T)<T\end{cases} \tag{1}$$

x direction

$$U_2(t)=\begin{cases}\dfrac{2U_{02}}{T}(t \bmod T) & 0\leqslant (t \bmod T)\leqslant \dfrac{T}{2}\\ 2U_{02}-\dfrac{2U_{02}}{T}(t \bmod T) & \dfrac{T}{2}<(t \bmod T)<T\end{cases} \tag{2}$$

where "mod" is the modulo operation. When the above signal is applied, the stack of two directions will output forces

$$F_1(t)=\frac{2nd_{33}U_1(t)K_sK_{b1}}{2K_{b1}+K_s} \tag{3}$$

$$F_2(t)=\frac{2nd_{33}U_2(t)K_sK_{b4}}{2K_{b4}+K_s} \tag{4}$$

where n is the number of layers of the piezoelectric stack and d_{33} is the piezoelectric coefficient.

Firstly, the vibration of the stator in the y direction is analyzed. In this model, the stiffness is constrained by $K_s<K_h\ll K_e$, and the stator will thus move as expected. Since there is $K_h\ll K_e$, the elastic beams e_1 and b_3 have little deformation which makes the displacement of m_3 small. Therefore, it has little influence on the vibration of two-degree systems m_1 and m_2. Thus the vibration equation can be written as

$$\begin{bmatrix}m_1 & 0\\ 0 & m_{21}\end{bmatrix}\begin{bmatrix}\ddot{y}_1(t)\\ \ddot{y}_2(t)\end{bmatrix}+\begin{bmatrix}K & -K\\ -K & K+K_h\end{bmatrix}\begin{bmatrix}y_1(t)\\ y_2(t)\end{bmatrix}=\begin{bmatrix}F_A(t)\\ F_B(t)\end{bmatrix}=\begin{bmatrix}F_1(t)-F_P-N-F_N(t)\\ -F_1(t)+F_P+N\end{bmatrix} \tag{5}$$

where $K=K_s+2K_{b1}$, it can be derived as

$$\begin{cases}y_1(t)=\dfrac{F_1(t)-F_P-N}{K}-\dfrac{F_N(t)}{K_h}\\ y_2(t)=-\dfrac{F_N(t)}{K_h}\end{cases} \tag{6}$$

where N is the external preload force, and $y_1(t)$ the y direction vibration equation of stator top.

The contact stiffness of stator and mover is written as K_C. When the voltage signal is applied on the structure, the force of the contact surface will be $N+F_N(t)$, where

$$F_N(t)=K_C y_1(t)=\frac{K_C K_h(F_1(t)-F_P-N)}{K(K_h+K_C)} \tag{7}$$

In the phase $t=kT$ to $t=kT+\Delta t$ (k is the nonnegative integer, $\Delta t \ll T$), $y_1(t)$ increases rapidly and the quantity is $K_C K_h U_{01}/[K(K_h+K_C)]$.

In the phase $t=kT+\Delta t$ to $t=kT+T/2$ (k is nonnegative integer, $\Delta t \ll T$), $y_1(t)$ remains unchanged.

In the phase $t=kT+T/2$ to $t=kT+T/2+\Delta t$ (k is the nonnegative integer, $\Delta t \ll T$), $y_1(t)$ reduced rapidly and the quantity is $K_C K_h U_{01}/[K(K_h+K_C)]$.

In the phase $t=kT+T/2+\Delta t$ to $t=kT$ (k is the nonegative integer, $\Delta t \ll T$), $y_1(t)$ remains unchanged.

To analyze the preload force, the whole preload force applied on the top of the stator is written as N_{total}. When there is single foot of stator works, N_{total} is

$$N_{total}=N+F_N(t) \tag{8}$$

As stiffness of external preload structure is bigger than the stiffness of internal structural, the y direction motion of stator in whole process barely changes. Therefore, the motion changes of y direction of stator in the drive and return phases are not obvious, which makes it difficult for the stator to separate completely from the mover in the return phase. When two driving feet of stator works alternately

$$N_{total}=N_1+F_{N1}(t)+N_2+F_{N2}(t) \tag{9}$$

When the double feet work alternatively, the sum of preload force of each stator $F_{N1}(t)+F_{N2}(t)$ keeps unchanged. This is because one foot staying at the drive phase can make another foot at the return phase achieve better separation, and thus the motor will attain good movement characteristics. The x direction motion characteristics of the stator is analyzed next and the lateral vibration characteristic can be written as

$$\begin{bmatrix} m_T & 0 \\ 0 & m_{22} \end{bmatrix}\begin{bmatrix} \ddot{x}_1(t) \\ \ddot{x}_2(t) \end{bmatrix}+\begin{bmatrix} K' & -K' \\ -K' & K'+K_h \end{bmatrix}\begin{bmatrix} x_1(t) \\ x_2(t) \end{bmatrix}=\begin{bmatrix} F'_A(t) \\ F'_B(t) \end{bmatrix}=\begin{bmatrix} F_2(t)-f(t) \\ -F_2(t) \end{bmatrix} \tag{10}$$

The motion characteristics of the stator in the x direction is further analyzed while the triangle-rectangle wave voltage signal is applied. If the stator separates completely in the return phase, it can be derived that

$$x_1(t)=\frac{F_2(t)}{K'}-\frac{f(t)(K'+K_h)}{K'K_h} \tag{11}$$

When $t \bmod T=T/2$ the x displacement has the maximum value. When the stator is at a steady state, the stator will drive the mover to move uniformly and linearly. At this time, with $f(t)=0$ the velocity of both mover and top of the stator can be derived as

$$x_1(t)=\frac{2n d_{33} U_{02} K_s K_{b4}}{K'T(2K_{b4}+K_s)}(t \bmod T)-\frac{f(t)(K'+K_h)}{K'K_h} \tag{12}$$

The motion displacement of the half period of the single stator is $x=v_x T/2$.

$$v_x=\frac{2nd_{33}U_{02}K_sK_{b4}}{K'T(2K_{b4}+K_s)} \tag{13}$$

During the return phase of one stator, another stator has just completed the return phase and start the driving phase. Thus the motion characteristics have no change.

If the stator is not separated completely in the return phase, the mover will still be in a uniformly linear motion relative to another stator when the system reaches the steady state. The force of the mover and double foot in the steady state is shown in Fig. 6.

Fig. 6 shows the situation that the right stator is in the driving phase and the left stator is in the return phase, where F_{11}, F_{12} are the output forces of the x direction stack of two stators, F_{K1}, F_{K2} are the resultant forces of elastic force in the motor process of stator, and f_1, f_2 the friction forces in contact point of stator and mover. As the mover is in a uniform linear motion, it can be derived that

$$f_1=f_2 \rightarrow \mu_1(N_1+F_{N1}(t))=\mu_2(N_2+F_{N2}(t)) \tag{14}$$

When stator 1 is in the return phase and stator 2 in the driving phase ($F_{N1}(t)<F_{N2}(t)$), it can be derived that $\mu_1>\mu_2$. If μ_0 is the dynamic friction coefficient and μ_{max} the maximum static

friction coefficient of the stator and mover, it can be drawn that $\mu_1=\mu_0$, $\mu_2<\mu_{max}$. As $F_N(t)$ has no change in the driving phase, the friction force of stator $f(t)$ in the driving phase is also a constant. Thus the velocity of mover remain stable in one period. From the above result, it is also shown that the external preload force has little influence on the motion characteristics of this kind of motor. If the load paralleled to the moving direction is applied to the mover, which is similar to the above analysis, it can be obtained that the movement characteristics of motor and the load applied to the mover is also irrelevant. This feature can be significantly improved the situation that the movement velocity reduces rapidly with the increase of load when using the ellipse trajectory to drive the mover .

To analyze some key point in one circle of stator, the motion mechanism can be shown as Fig. 7.

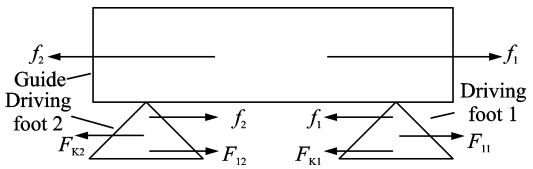

Fig. 6 Forces in the x direction

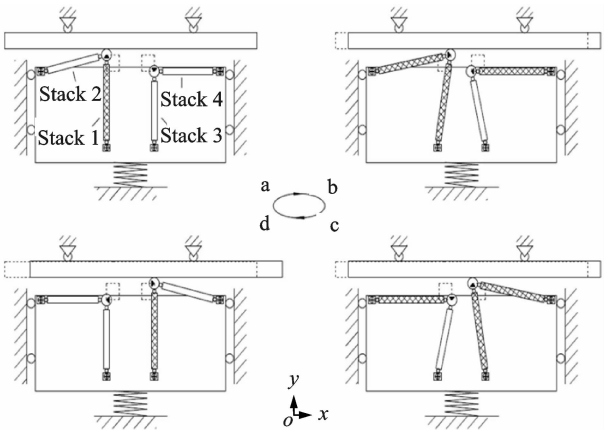

Fig. 7 Driving process of the proposed linear motor

There are four working phases of the motor in Fig. 7, where, "a" and "c" represent the moments of $t=0$ and $t=T/2$, while "b" and "d" represent the previous moments of $t=T/2$ and $t=T$. To describe the working process, piezoelectric stacks 1 and 2 are defined in Fig. 2 and piezoelectric stacks 3, 4 are similar as stacks 1, 2 on another layer of the stator.

(1) In the first phase "a", the piezoelectric stack 1 extends in the y direction with a voltage applied on it. At this moment, the left stator driving foot pushes the mover.

(2) In the second phase "b", the piezoelectric stacks 2, 4 extend a micro length δ in the x direction and negative x direction. From phase "a" to phase "b", the left stator driving foot drives the mover to move displacement δ in the x direction.

(3) In the third phase "c", the piezoelectric stack 1 returns to the original length. At the same time, the piezoelectric stack 3 extends in the y direction with an applied voltage. Thus the right stator driving foot pushes the mover.

(4) In the fourth phase "d", the piezoelectric stacks 2, 4 extend a micro length δ in the negative x direction and x direction. From phase "c" to phase "d", the right stator driving foot drives the mover to move displacement δ in the x direction.

In a circle, the stator pushes the mover to move displacement 2δ in the x direction. By repeating Steps (1) to (4), the motor will move linearly and continuously.

1.3 Simulation analysis

In the stator structure shown in Fig. 3, piezoelectric stack is selected as the driving element. In other parts of the structure, 45 steel is utilized. ANSYS is used to perform the finite element method (FEM) analysis. The simulation model of the stator is shown in Fig. 8. The experiments of the piezoelectric stack show that the displacement of the stack is in a linear relationship with the voltage of input signal and it barely has relationship with the frequency of input signal. When the input signals shown in Fig. 9 are applied to four piezoelectric stacks, the trajectory of the top of the driving foot is shown in Fig. 10. Through the way, two layers of the stator move alternatively, and the mover will move linearly. Ceramic materials are used as the contact surface of the stator and mover. Applied an appropriate preload force between the stator and the mover,

dynamic simulation is performed under different voltages and frequencies.

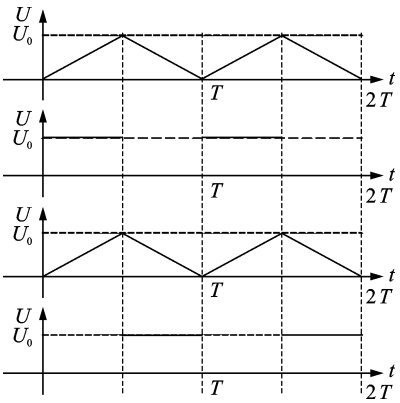

Fig. 8 Periodic voltage signals applied to four stacks

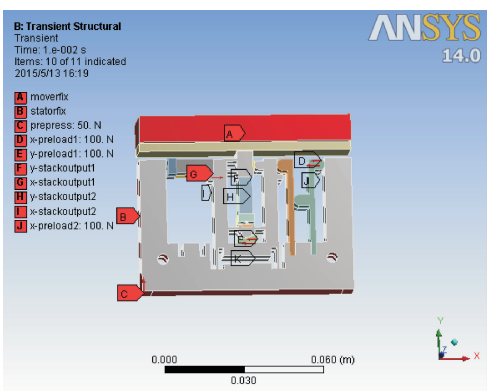

Fig. 9 Simulation model of the stator

From the trajectory of the top of stator in Fig. 9, when 100 V, 100 Hz voltage signal is applied, to the stack, the top of stator is in a rectangular movement. Also the relationship of movement displacement versus time is shown in Fig. 10. Fig. 11 shows the mover is in uniformly linear motion.

When voltage and frequency of the signal applied to the motor is changed, the relationship between the velocity of mover and voltage and frequency of the signal is shown in Fig. 12.

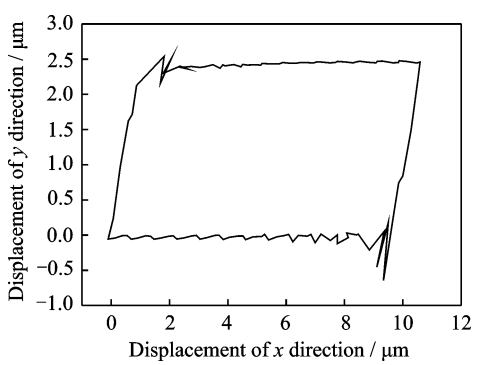

Fig. 10 Simulation locus of the driving foot top end

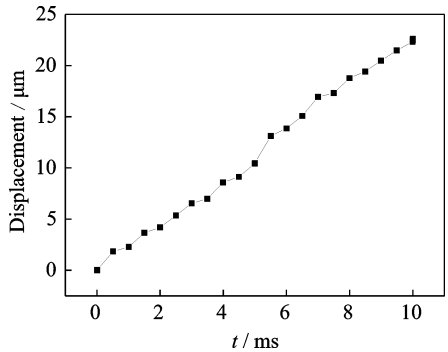

Fig. 11 Curve of displacement of mover versus time

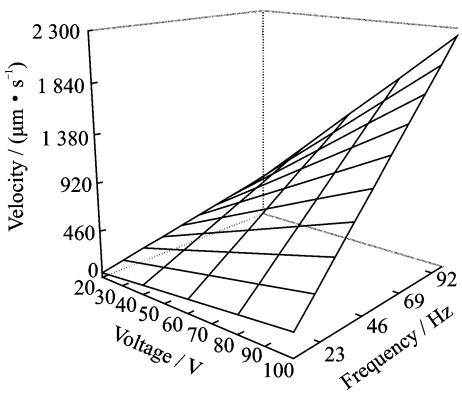

Fig. 12 Curve of velocity versus voltage and frequency

From the simulation results, it can be concluded when rectangle-triangle wave signal is applied to the stacks, the movement locus of two driving feet is rectangle and two feet drive the mover to linearly move by friction. Furthermore, the velocity of mover has a linear relationship with the voltage and frequency of the applied signal.

2 Experiments

A series of experiments are conducted to validate the working principle and to evaluate the characteristics of the motor.

2.1 Experiment system

To test this structure, the motor prototype is assembled as shown in Fig. 13. Four piezoelectric stacks NAC2013-H14 produced by noliac company is used in the structure. The driving signal is applied by the signal generator and the power amplifier. This signal is displayed on the oscilloscope and also applied on the stacks of the

motor, which ensures the motor in an operative mode. The displacement of the motor can be measured by the laser sensor LK-H020 from Keyence Company with the resolution of 1 nm.

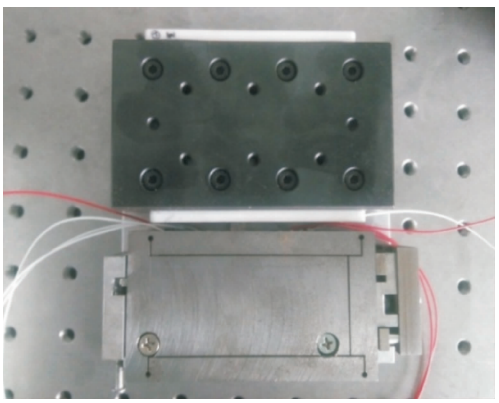

Fig. 13 Prototype of motor

2.2 Performance test

Firstly, applying rectangle-triangle signal with different frequency and voltage on the four stacks to perform the characteristics test. The results are shown in Fig. 14.

In Fig. 14(a), there is a linear relationship between the voltage of signal and the velocity of the motor. The relationship between the frequency of the signal and the velocity of the motor is shown in Fig. 14(b), from which it can be seen that two parameters nearly have a linear relationship. With a frequency of 120 Hz and a voltage of 120 V, the velocity reaches 670.22 μm/s. When the frequency of the signal continues increasing, the motion of the motor will be more complex. Affected by the hysteresis effect of the stacks, it would not be in the motion as expected.

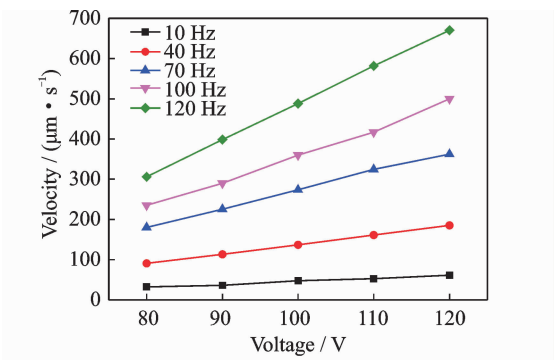

(a) Velocity of the motor versus voltage by different frequencies

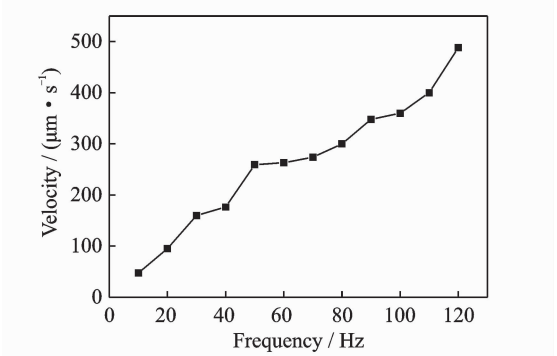

(b) Velocity of the motor versus frequency with 100 V voltage

Fig. 14 Results of characteristics test

As load capacity is also an important factor, a load experiment is conducted by using the motor to pull the weights. The results are shown in Fig. 15. Fig. 15 shows that the velocity of the motor reduces when the load increases. With a voltage of 100 V, the maximum load is 3 N. Since the frequency used in the experiments is low (0—200 Hz), the load capacity is not very strong.

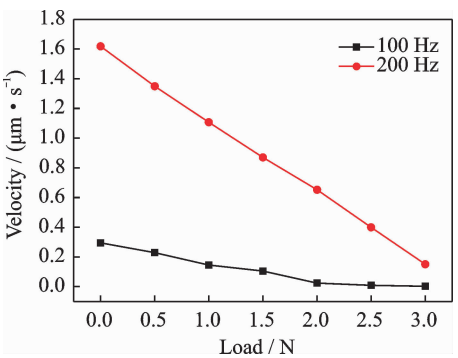

Fig. 15 Velocity of motor versus load with 100 V voltage

As the guide of this motor has enough space to bear something, the bearing capacity is tested by putting weight on the guide of the motor. The results are shown in Fig. 16.

When the weight increases to 20 N with a frequency of 10 Hz and a voltage of 100 V, the velocity has little change. It shows that the bear-

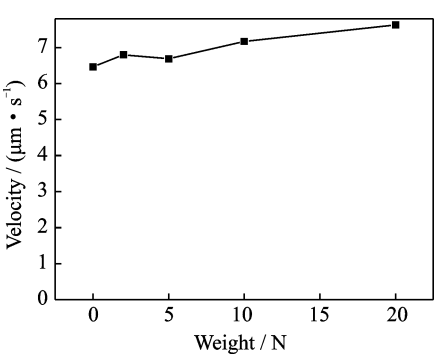

Fig. 16 Velocity of motor versus weight with 100 V voltage

ing capacity of the motor is strong. So this motor can be stacked one by one to realize multi-degree of freedom of movement.

To test the step distance of the motor, several pulse signals with different signals are applied on the piezoelectric elements. The results are shown in Fig. 17.

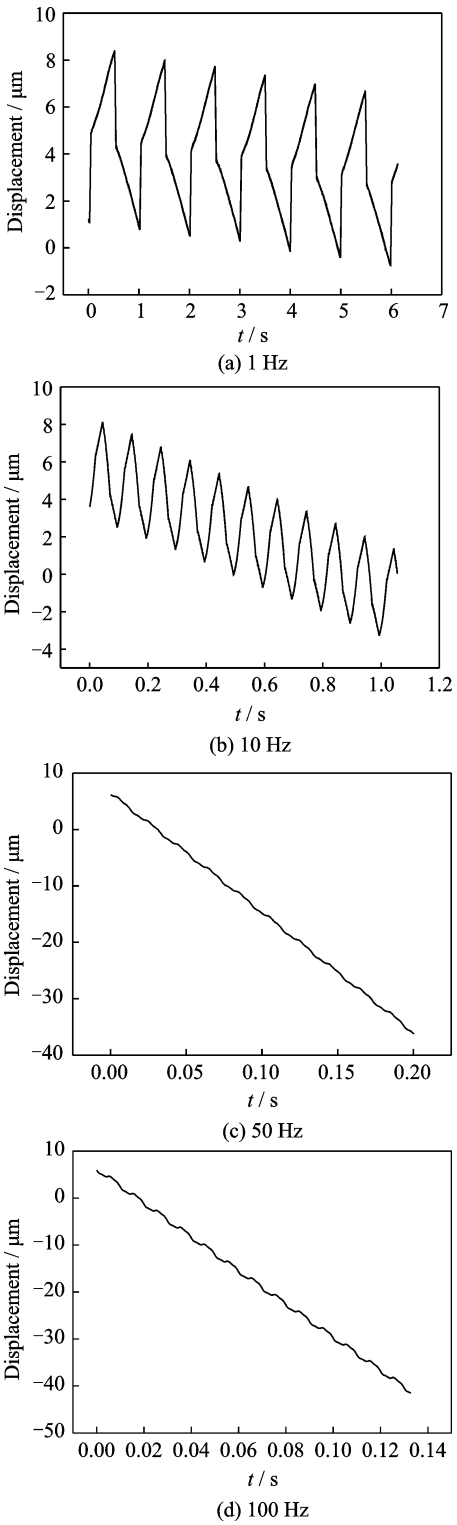

Fig. 17 Displacement-time curve with different frequencies

With frequencies of 1, 10, 50, 100 Hz and a voltage of 100 V, the displacement-time curves are shown in Fig. 17. When the frequency are 1, 10, 100 Hz, the stepping distances are 0.35, 0.65, 3.57, 3.61 μm in average, respectively. Theoretically, the step distance will not change with the frequency shift. But there is a little different on the contact situation of two driving foot with the mover, it will lead to a large error in motion of every step. Meanwhile, the curve indicates that the difference on the contact situation will have a smaller effect on the motion of the motor when frequency increases. So the step distance should be described as 3.6 μm with a voltage of 100 V.

3 Conclusions

A double-foot alternate stepping piezoelectric linear motor is proposed. The motor working on the basis of non-resonant principle utilizing piezoelectric stack can achieve large stroke as well as high precision. Triangle-rectangle wave signal is applied to the four piezoelectric stacks of two-layer of the stator to achieve step actuation mode. Kinematics model of the stator is established to analyze the operation mechanism of this motor. Also, displacement, velocity and output force are analyzed theoretically to find some general law of the motor. FEM analysis manifests the characteristics with driving signal applied. With the holding structure and the preload structure of the motor designed, a prototype is fabricated to verify the feasibility of the motor. In the performance test, the following results are concluded:

(1) There is a linear relationship between frequency (or voltage) of the signal and the velocity of the motor. With a frequency of 120 Hz and a voltage of 120 V, the velocity reaches 670.22 μm/s.

(2) Load experiment shows that the velocity of the motor reduces when the load increases. With a voltage of 100 V, the maximum load is 3 N. And the load capability is not strong because the working frequency is low (0—200 Hz). Furthermore, the bearing capability is tested. When

the weight increases to 20 N with a frequency of 10 Hz and a voltage of 100 V, the velocity barely changes, which indicates that the bearing capacity of the motor is strong.

(3) As the motor works by double-foot alternate stepping motion, the stepping distance is measured using the laser sensor. With a voltage of 100 V, the stepping distance is averagely 3.6 μm.

Acknowledgements

This work was supported by the National Natural Science Foundations of China (Nos. 51505161, 51375224), and the Guangzhou Municipal University Research Projects (No. 1201610315).

References:

[1] YOON M, KHANSUR N H, LEE K, et al. Compact size ultrasonic linear motor using a dome shaped piezoelectric actuator[J]. Journal of Electroceramics, 2012, 28(2/3): 123-131.

[2] SHI Y L, ZHAO C S. Simple new ultrasonic piezoelectric actuator for precision linear positioning[J]. Journal of Electroceramics, 2012, 28(4): 233-239.

[3] SHI Y L, ZHAO C S. A new standing-wave-type linear ultrasonic motor based on in-plane modes[J]. Ultrasonics, 2011, 51(4): 397-404.

[4] NEWTON D, GARCIA E, HORNER G C. A linear piezoelectric motor[J]. Smart Materials & Structures, 1998, 7(3): 295-304.

[5] CHEN Q W, JU Q Y, HUANG W Q, et al. Stick-slip tower-shaped piezoelectric actuator[J]. Transactions of Nanjing University of Aeronautics and Astronautics, 2015, 32(2): 156-162.

[6] CHEN Q W, SHI Y L, HUANG W Q. Single-mode-drive-type bi-directional linearly moving ultrasonic motor with inclined slider and V-shaped stator [J]. Journal of Nanjing University of Aeronautics & Astronautics, 2015, 47(1): 139-144. (in Chinese)

[7] SHI Y L, LI Y B, ZHAO C S. Optimum design of a linear ultrasonic motor based on in-plane modes[J]. Proceedings of the CSEE, 2008, 28(30): 56-60.

[8] LI J, SEDAGHATI R, DARGAHI J, et al. Design and development of a new piezoelectric linear Inchworm (R) actuator[J]. Mechatronics, 2005, 15(6): 651-681.

[9] CHEN Q F, YAO D J, KIM C J, et al. Mesoscale actuator device: Micro interlocking mechanism to transfer macro load[J]. Sensors and Actuators A—Physical, 1999, 73(1/2): 30-36.

[10] RENNER C, NIEDERMANN P, KENT A D, et al. A vertical piezoelectric inertial slider[J]. Review of Scientific Instruments, 1990, 61(3): 965-967.

[11] NIEDERMANN P, EMCH R, DESCOUTS P. Simple piezoelectric translation device[J]. Review of Scientific Instruments, 1988, 59(2): 368-369.

[12] POHL D W. Dynamic piezoelectric translation devices[J]. Review of Scientific Instruments, 1987, 58 (1): 54-57.

[13] CHEN X F, LIANG Y, HUANG W Q, et al. Vibration characteristics analysis for the stator of dynamic friction linear piezoelectric stack motors[M]// Applied Mechanics and Materials. Stafa-Zurich: Trans Tech Publications LTD, 2014: 442, 392-396.

[14] CHEN X F, WANG Y, SUN M X, et al. Linear piezoelectric stepping motor with broad operating frequency[J]. Transactions of Nanjing University of Aeronautics and Astronautics, 2015,32(2):137-142.

[15] LIU W H, WANG Y, HUANG W Q, et al. A linear stepping piezoelectric motor using inertial impact driving[J]. Applied Mechanics and Materials, 2012, 226/227/228: 693-696.

[16] PAN S, HUANG W Q, WANG Y, et al. High efficiency driving of linear motor based on piezoelectric actuator[J]. Optics and Precision Engineering, 2011, 19(10): 2464-2471.

Mr. **Sun Mengxin** received his B. S. Degree in flight vehicle design and engineering from Nanjing University of Aeronautics and Astronautics in 2012. He is currently a Ph. D. candidate in mechanical design and theory at Nanjing University of Aeronautics and Astronautics. His research interest focuses on piezoelectric motor technology and precision drive technology.

Prof. **Huang Weiqing** received his Ph. D. degree in Mechanical Engineering from Hong Kong University of Science and Technology in 1999. He is currently a professor of School of Mechanical and Electric Engineering in Guangzhou University. His research interests include the piezoelectric precision driving technology and vibration utilization technology.

Dr. **Wang Yin** received his Ph. D. degree in Mechanical Design and Theory from Nanjing University of Aeronautics and Astronautics in 2014. He is currently a lecturer at Center for precision Measurement Technologies and Instruments in Huaqiao University. His research interests include the piezoelectric actuators and Ultrasonic machining.

Mr. **Lu Qian** received his M. E. degree in Mechanical electronic engineering from China University of Mining and Technology in 2009. He is currently an associate professor at School of Mechanical Engineering in Yancheng Institute of Technology. His research interests include the Precision driving and Automatic control system.

(Production Editor: Zhang Tong)